10-16-2008

Helical Peptides Derived from Lactoferrin Bind Hepatitis C Virus Envelope Protein E2

Reem Beleid
University of Alberta

Donna Douglas
University of Alberta

Norman Kneteman
University of Alberta

Kamaljit Kaur
Chapman University, kkaur@chapman.edu

Recommended Citation

Beleid R, Douglas D, Kneteman N, Kaur K. Helical peptides derived from lactoferrin bind hepatitis C virus envelope protein E2. *Chem. Biol. Drug Des.* 2008;72(5):436-443. doi: 10.1111/j.1747-0285.2008.00715.x

Helical Peptides Derived from Lactoferrin Bind Hepatitis C Virus Envelope Protein E2

Helical Peptides derived from Lactoferrin bind Hepatitis C Virus Envelope Protein E2

Reem Beleid[⊥], Donna Douglas[#], Norman Kneteman[#], Kamaljit Kaur*[⊥],

[⊥] *Faculty of Pharmacy and Pharmaceutical Sciences, University of Alberta, Edmonton, AB, Canada, T6G 2N8 and* [#] *Department of Surgery, Faculty of Medicine and Dentistry, University of Alberta, Edmonton, AB, Canada, T6G 2B7*

* To whom correspondence should be addressed. Phone: 780-492-8917; Fax: 780-492-1217; E-mail: kkaur@ualberta.ca

Keywords: HCV; Envelope protein E2; Lactoferrin-derived peptides; Protein-peptide interaction

Abstract

Hepatitis C virus (HCV) is a major cause of chronic hepatitis, liver cirrhosis, and hepatocellular carcinoma infecting more than 170 million people. HCV envelope glycoprotein E2 binds several cell surface molecules that act as receptor candidates mediating HCV entry into hepatocytes. Peptides derived from human lactoferrin (LF) have been shown to bind HCV E2 protein thereby preventing HCV entry in cultured hepatocytes. In this study, starting from a 33-residue human LF-derived peptide, a number of biotin-linked α-peptides were synthesized and investigated for their E2 protein binding activity. E2 protein from HCV genotype 1b was expressed in 293 human embrionic kidney cells and purified using affinity chromatography. A biotin-streptavidin based binding assay was developed to determine the binding affinity of the synthetic peptides for E2 protein. Two of the peptides bound E2 specifically with submicromolar to low micromolar affinity (equilibrium dissociation constant, K_d, of 0.569 and 28.8 μM). Further, these two peptides had the highest helical content in solution as observed by CD spectroscopy, suggesting that binding affinity increases with increase in helicity. These results have provided new lead peptides for future investigations of HCV entry inhibitors that may provide an interesting approach to prevent HCV infectivity.

Abbreviations: aa, amino acid; CD, circular dichroism; E2, HCV envelope 2 glycoprotein; HCV, hepatitis C virus; HOBt, 1-hydroxybenzotriazole; HRPO; horseradish peroxidase; K_d, equilibrium dissociation constant; LF, lactoferrin; MALDI-TOFMS, matrix-assisted laser desorption ionization time-of-flight mass spectrometry; Ni^{2+}-NTA, nickel(II)-nitrilotriacetic acid; SDS-PAGE, sodium dodecyl sulfate-polyacrylamide gel electrophoresis; SPPS, solid-phase peptide synthesis; TFA, trifluoroacetic acid; TMB, 3,3',5,5'-tetramethylbenzidine

Introduction

Hepatitis C infection has become a "silent pandemic" around the globe infecting more than 170 million people worldwide (1). It is estimated that three to four million persons are newly infected each year, 70 percent of whom will develop chronic hepatitis. HCV is responsible for 50–76 percent of all liver cancer cases, and two thirds of all liver transplants in the developed world (2). There is no vaccine for HCV and the current most effective therapies for HCV infection involve treatment with pegylated α-interferon, either alone or in combination with antiviral agent ribavirin. Although this combination therapy has led to a dramatic improvement in the treatment outcome, the low efficacy of the therapy (response rate ~ 50%) along with resistance problems, poor tolerability, and high cost necessitates exploration of new and more effective therapies (3, 4).

Currently, the principal targets of new antivirials are the NS3 protease and the RNA-dependent RNA polymerase (RdRp) (5). More recently, cyclophilin inhibitors that target host-virus interactions have also gained attention (6). Several molecules inhibiting these targets are currently in either preclinical or clinical stages. The early steps of the HCV life cycle are also attractive targets for novel therapies, such as virus attachment to host cells, internalization of the virus-receptor complex, and the fusion that releases the nucleocapsid into the cytoplasm. However, the later targets have been less explored (7, 8). Although the entry mechanism of HCV remains unclear, it has become evident that the initiation of the infection takes place by association of the viral envelope protein E2 with specific cell-surface receptor(s) (9). Many groups have demonstrated that the truncated soluble versions of E2 bind specifically to human cells. This glycoprotein is used to identify interaction with cell-surface receptors, such as, CD81, SR-B1, LDL, DC-SIGN and L-SIGN. Inhibition of this interaction between E2 and the cell-

surface receptors has therefore been identified as a possible target for designing anti-HCV molecules.

Several groups have designed small molecules that inhibit binding of HCV-E2 to CD81 (10, 11). Molecules with bis-imidazole scaffold as mimics of helix D of CD81 were found to inhibit binding of HCV-E2 to CD81 (11). A variety of amine complexes with 1-boraadamatane, namely, amantidine analogues showed antiproliferative effect on CD81-enriched cell lines (12). Recently, an oral antiviral arbidol, an indole derivative has been shown to inhibit HCV entry via HCV pseudoparticles (HCVpp). Arbidol inhibited HCVpp-mediated membrane fusion in a dose-dependent manner in different HCV genotypes, namely, 1a, 1b, and 2a (13). Furthermore, carbohydrate-binding agents (CBAs) derived from different prokaryotic and plant lectins have antiviral activity due to their carbohydrate-binding properties. These agents interact with the viral envelope glycoprotein and efficiently prevent the HCV entry process (14).

Two peptides derived from cyanobacterium and human lactoferrin (LF) have been reported as HCV entry inhibitors (15, 16). Cyanovirin-N, a 101-residue peptide (11 kDa), from cyanobacterium *Nostoc ellipsosporum* has been shown to inhibit HCV entry by binding to the envelope protein. Cyanovirin-N shows broad inhibitory effect against various genotypes in nanomolar concentrations. The mode of action is thought to be through interaction with N-glycans of the E2 protein preventing E2 binding to the CD81, consequently blocking HCV entry to the target cell (15). Another peptide derived from the C-terminal region of human LF showed binding activity to HCV-E2, leading to the inhibition of HCV infection in the target cells (16). Using a cell-based assay, it was shown that 33-residue LF fragment or *Nozaki peptide* (Figure 1) specifically prevented HCV infection in human hepatocytes. Furthermore, the Nozaki peptide did not bind the hyper variable region (HVR-1) located at the N-terminal of E2 protein (384-

415). The authors demonstrated that the mechanism of action of this peptide fragment is by binding to the E2 protein of HCV, thereby blocking its entry into the host cell, rather than binding to the host cell-surface receptors (16). The Nozaki peptide, however, was found to possess weaker E2-protein binding activity and anti-HCV activity to that of human LF.

Figure 1: (A) Three-dimensional structure of 33-residue lactoferrin-derived peptide (600-632 amino acids) obtained from the crystal structure of recombinant human lactoferrin (pdb 1CB6) (17). Structure is shown as a ribbon diagram highlighting the helical (red) secondary structure. (B) Amino acid sequence of the 33-residue lactoferrin-derived peptide. Helical residues are underlined.

We have studied five peptides (**1-5**, Figure 2) derived from the C-terminal region of LF sequence based on the results of Nozaki and coworkers (16). These peptides were designed to identify a lead peptide with stronger binding affinity to E2. E2 from HCV genotype 1b was expressed in mammalian cells and purified using affinity chromatography. The results of the binding affinity between peptides **1-5** and the E2 protein, as well as, their mechanism of binding are reported here.

Figure 2: Sequence of five lactoferrin-derived peptides synthesized and studied herein. Residues that are underlined indicate a change from the native lactoferrin sequence. Nle stands for norleucine and b denotes biotin covalently linked to the N-terminus of the peptides.

Results and Discussion

Design and Synthesis of Peptide Ligands

It was observed from the three-dimensional crystal structure of recombinant lactoferrin (17) that the 33-residue LF fragment or the Nozaki peptide is present on the surface of the protein. Furthermore, the crystal structure shows that the 33 amino acid region (aa 600-632) consists of a central helical region (aa 607-620) and two flexible loops on the sides as shown in Figure 1. Based on these observations, we decided to synthesize peptides containing the central helical region (i) with both the N- and C-terminal loops, (ii) with the C-terminal loop, and (iii) without loops (Figure 2). Peptide **1**, a 33-residue peptide with the central helical region and both the loops, is same as the Nozaki peptide except with a mutation at methionine 604 and with biotin (MW 361) covalently attached at the N-terminus. In contrast, the Nozaki peptide has maltose-binding protein (MW 44000) covalently attached to it. Peptides **2** and **3**, consisting of 27 and 17 amino acids, have either N-terminal loop or both N- and C-terminal loops deleted, respectively. Finally, peptides **4** and **5** were designed with binding enhancing mutations (16). Peptides **4** and **5** are same as peptides **1** and **2** but with two mutations each, namely, S626A and D630A.

Peptides **1**-**5** (Figure 2) derived from the C-terminal region of human lactoferrin were synthesized manually on Wang resin using standard Fmoc solid-phase peptide synthesis (SPPS) as described previously (18). HBTU or BOP and HOBt were used as coupling agents. For peptides **1** and **4**, methionine (Met) was replaced by norleucine (Nle) in order to avoid any oxidation problems. After the final N-terminal Fmoc amino acid was coupled to the peptide-resin, the Fmoc group was removed and the N-terminus was biotinylated as described in the

Methods section. Crude peptides were purified on a semi-preparative reversed-phase HPLC column by either isocratic or a gradient elution method using acetonitrile and water as solvents. The mass of the crude and pure peptides were confirmed by MALDI-TOF mass spectrometry. Purity of the peptides was confirmed by analytical reversed-phase HPLC and mass spectrometric analysis. The yield of the purified peptides ranged between 50-65%. The biotinylated peptides were used to develop a biotin-streptavidin based binding assay for the evaluation of binding affinity of these peptides toward the E2 envelope protein.

Expression and Purification of E2 glycoprotein

The HCV envelope E2 glycoprotein, exposed on the surface of virions, is likely to be involved in the interactions with the host and has been identified as responsible for binding of HCV to target cells (19). HCV-E2 binds with high affinity to target cells only when expressed in mammalian cells, which is most likely due to the N-glycosylation and conformational changes it undergoes when expressed specifically in mammalian cells. To study interaction of E2 protein with the synthesized peptide ligands, we expressed the extracellular (soluble) domain of E2, corresponding to aa 384-661 of isolate N2 (1b subtype) fused to a six-histidine tag at the C-terminus. Human embrionic kidney (HEK) 293 cells were transfected with plasmid vector E2N2661 using Lipofectamine 2000, and the protein was harvested after 48 hr. The expected molecular weight of the glycosylated E2 protein is in the range of 62-66 kDa depending on glycosylation sites (20). Western blot analysis of the expressed protein suggested the expression of E2 protein with MW ~63 kDa (Figure 3).

The expressed E2 protein contains a His tag at the C terminus which facilitates purification using a nickel nitrilotriacetic acid (Ni^{2+}-NTA) resin column. The crude cell lysate

containing the His-tagged E2 protein was incubated with the Ni^{2+}-NTA resin allowing non-covalent binding of the protein to the resin. The resin was then washed thoroughly to remove any unbound impurities and the pure protein was eluted with high concentration of imidazole (300 mM, elution buffer). The Western blot analysis using anti-E2-mAb and anti-His6-mAb showed that the fractions 3-8 contained pure protein (Figure 3). These six fractions containing the highest concentrations of the pure protein were combined and dialyzed against PBS to obtain 7.8 mL of E2 with a concentration of 16.6 μg/mL.

Figure 3: E2N purification: Western blot analysis of the fractions obtained from the IMAC column, probed with mouse anti-His6 (1:1000) (left) and mouse anti-E2 (1:20) (right) monoclonal antibodies. CL: crude lysate; FT: flow through; 3-8: fractions 3-8 obtained using the elution buffer.

Binding of Lactoferrin-derived Peptides to E2 Protein

A biotin-streptavidin based binding assay was developed to access the binding affinity of the lactoferrin-derived synthetic peptides for E2 glycoprotein. In this assay, biotin-labeled peptides bind to E2 protein allowing detection of the E2-bound peptides using a strepavidin-horseradish peroxidase (Strep-HRPO) conjugate. At the end of the assay, absorbance of the TMB substrate for Strep-HRPO is observed at 650 nm. All the five peptides (**1**-**5**) displayed concentration-dependent response of peptide binding to E2 protein. During the assays, biotin without the peptide was used as a control. Biotin (4-40 μM) showed no binding to the E2 protein. Also, peptides **1**-**5** did not bind to BSA when used as a control protein. For each

peptide, the binding assay was repeated at least 3-4 times. It was suggested by Nozaki *et al*. that the lactoferrin-derived peptides bind to a single site on the surface of the E2 protein (16). Based on this hypothesis, it was assumed that all the peptides will display binding curves following the Scheme 1,

Scheme 1

$$P + L \underset{K_d \text{ dissoc.}}{\rightleftharpoons} PL$$

where P = E2 protein, L = ligand or peptide, and PL = noncovalent protein-peptide adduct. Initial glance at the binding curves showed that peptides **3** and **5** displayed an exponential rise in absorbance with increasing peptide concentration (Figure 4). However, peptides **1**, **2**, and **4** displayed a more complex mechanism of binding. These peptides show an initial lag in the binding curve suggesting non-specific binding or multiple binding sites for the peptide ligands on E2 protein (Figure 5).

Figure 4: Binding of E2 protein to peptides **3** (top) and **5** (bottom). Shown is absorbance of TMB substrate at 650 nm as a function of different peptide concentration. The symbols are experimental data points whereas the line was calculated by fitting the data to Scheme 1 as described in the text.

Accordingly, the data for peptides **3** and **5** were fitted to Scheme 1 to obtain the hyperbolic curves as shown in Figure 4. The fitted curves and the values for the corresponding equilibrium dissociation constants (K_d) were obtained by the DynaFit program (21, 22) as

described previously (23). DynaFit is a numerical simulation software that allows nonlinear least-squares regression of the equilibrium or kinetic data to obtain binding constants. Using this program, K_d values of 28.8 ± 2.90 and 0.569 ± 0.0390 μM were obtained for peptides **3** and **5**, respectively. Peptide **5** with two mutations (S626A and D630A) displayed better binding profile compared to all other peptides including the 33 residue peptide **1**. Single mutation of S626 or D630 to alanine in the 33 residue Nozaki peptide was previously found to enhance binding affinity.(16) Our results further confirm that these mutations augment binding activity.

Figure 5: Binding of E2 protein to peptides **1** (Δ), **2** (□), and **4** (o). Shown is absorbance of TMB substrate at 650 nm as a function of different peptide concentration. The symbols are experimental data points whereas the line is drawn to guide the eye.

Circular Dichroism of α-Peptides

Circular dichroism (CD) spectroscopy was used to evaluate the secondary structure of the synthetic peptides in solution. CD spectra were obtained for three different concentrations (25, 50, and 100 μM) in phosphate buffer (pH 7.4) for each peptide. The spectra were found to be independent of concentration suggesting no aggregation in this concentration range. In all the peptides, helical structure was induced indicated by the appearance of distinct negative bands at 206-207 nm and negative shoulders near 220 nm. The CD spectra were analyzed using CDPro software (24) to obtain relative ratio of different secondary structures present as described previously (Table 1) (18). Quantitative analysis of the distribution of secondary structure

showed that peptides **3** and **5** have high helical content of 38 and 71%, respectively. Both the 33-residue peptides, **1** and **4,** displayed similar secondary structure with about 32-34% α-helix. Surprisingly, peptide **2** with 27 amino acids, same length as peptide **5**, showed substantial loss of the α-helical structure. The helical conformation (44% helical) in **2** could be induced in the presence of 50% trifluoroethanol. It is, however, noteworthy that peptides **3** and **5** have the highest helical content (Table 1), with **5** exhibiting greater helicity than **3**. This helical region may be crucial for binding as pointed out by Nozaki and coworkers (16). The binding affinity (K_d) of **5** and **3** was 0.569 μM and 28.8 μM, respectively. This suggests that increasing the helical content or stabilizing the helical conformation may lead to enhanced binding activity.

Table 1: CD Analysis of the Secondary Structure Fractions of Peptides **1-5** in PBS at 25 °C.

Peptides **1-5** derived from LF contain several charged and polar residues with an overall charge of +3 or +4. The α-helical wheel representation of peptide **5** shows that the peptide is amphipathic with a polar/hydrophilic and hydrophobic face (Figure 6). This was further supported by the very high amphipathicity value of 7.65 for peptide **5**. Amphipathicity was determined by the calculation of hydrophobic moment (25) using the software package Jemboss version 1.5 (26). The amphipathic nature of the peptide suggests that the predominant interaction involved between the peptide and E2 is electrostatic and hydrogen bonding interaction. Further, it is presumed that peptides **1-5** do not bind the hypervariable region 1 region (aa 384-410) of the E2 protein, since the 33-residue Nozaki peptide preferentially bound to aa 411-500 of the E2 protein (16). This binding site on E2 also seems different from the

CD81 binding site. CD81 is known to recognize aa 480-493 and aa 544-551 of the E2 protein (27). E2 is a heavily glycosylated protein and its three-dimensional structure is not yet elucidated (28, 29). Therefore, the spatial relationship between the LF-derived peptides and E2 binding site is not known. It is however clear from our binding assay results that **3** and **5** bind on a single site on E2. Peptides **1**, **2**, and **4** may bind on multiple sites on E2 protein indicated by the different binding rate constants. These multiple sites could be in close proximity to the primary binding site, as tandem repeats of the Nozaki peptide were found to enhance binding activity (30). Abe and coworkers found that the E2 binding activities of the two repeats (33-residue Nozaki peptide)$_2$ and the three repeats (33-residue Nozaki peptide)$_3$ were stronger than the Nozaki peptide itself (30).

Figure 6: Edmundson α-helical wheel representation of peptide **5**. The solid curve indicates the polar/hydrophilic face and the dashed curve denotes hydrophobic face.

Evaluation of a relatively small number of α-peptides has allowed identification of potent and specific binders of E2 that are suitable candidates for further investigation. These peptides are currently being evaluated using a cell-based anti-HCV assay and will serve as lead molecules for the design of future peptide-based or peptidomimetic libraries. Such molecules, useful for the elimination of circulating HCV, can be used as prophylactic alone or in combination with other anti-HCV agents. It has been suggested that a cocktail of drugs targeting multiple steps of the HCV life-cycle will be required to treat chronic hepatitis C (31).

In summary, we have reported five peptides (**1**-**5**) derived from LF sequence that bind to E2 protein from the N strain of HCV in a concentration-dependent manner. Two of the peptides

identified, **3** and **5**, bind E2 with submicromolar to micromolar affinity. These two peptides are smaller in length than the starting 33-residue LF-derived peptide, and contain the central helical region from the parent peptide. Further, among the five peptides evaluated for binding E2, **3** and **5** had the highest helical content (38% and 71%, respectively) demonstrating the importance of helical secondary structure for binding. These peptides will serve as lead for our future investigations of HCV entry inhibitors. Based on these results, several libraries of peptides and peptidomimetics are currently being designed and synthesized that will serve as tools for understanding the molecular basis of E2 and cell surface receptor interactions, and may lead to a feasible approach for the treatment and prevention of HCV infection.

Materials and Methods

All commercially available solvents and reagents were used without further purification. D-Biotin was purchased from Sigma Chemical Co. (St. Louis, MO, USA). Wang resin and BOP were obtained from Novabiochem (San Diego, USA). HOBT, HBTU, and Fmoc-protected amino acids were purchased from Peptides International (Louisville, USA). RP-HPLC purification and analysis were carried out on a Waters (625 LC system) HPLC system using Vydac semi-preparative C18 (1 x 25 cm, 5 μm) and analytical C8 (0.46 x 25 cm, 5 μm) columns. Compounds were detected by UV absorption at 220 nm. Mass spectra were recorded on a MALDI Voyager time-of-flight (TOF) spectrometer (VoyagerTM Elite).

Plasmid vector E2N2661 (genotype 1b isolate N2), with a concentration of 10 μg/μL was provided by IRBM (Merck, Italy) (29). Lipofectamine 2000, 0.05% Trypsin / EDTA, OptiMEM-I, and nitrocellulose membrane were purchased from Invitrogen (Carlsbad, Canada). Human embrionic kidney (HEK) 293 cells were obtained from American Type Tissue Culture

(Bethesda, MD, USA). Kanamycin, bovine serum albumin (BSA), agarose, 2-mercaptoethanol, imidazole and Folin-phenol were purchased from Sigma Chemical Co. (St. Louis, MO, USA). Equipment and reagents for SDS-PAGE and Western blotting were from Bio-Rad (Mississauga, Canada). Dulbecco's Modified Eagle's Medium (DMEM) and fetal bovine serum (FBS) were purchased from Gibco BRL (Burlington, Canada). The anti-His_6 mouse monoclonal antibody was purchased from Novagen (Madison, USA), whereas the anti-HCV-E2 mouse monoclonal antibody was purchased from ViroStat (Portland, ME). Restriction endonucleases *Hind*III was obtained from Life Technologies (Burlington, Canada). Plasmid Mega Kit, plasmid mini-preparation kit and Ni–NTA–agarose resin was obtained from Qiagen (Mississauga, Canada). Enhanced chemiluminescence (ECL) immunodetection kits, antimouse horseradish peroxidase-linked secondary antibodies and DNA molecular weight markers were purchased from Amersham Biosciences (Oakville, Canada). TMB (3,3',5,5'-tetramethylbenzidine) substrate solution was obtained from KLP Laboratories (Gaithersburg, USA).

Peptide Synthesis

Stepwise synthesis of the peptides **1-5** was done manually on a 0.3-mmol scale of Wang resin (1.0% DVB cross-linked) following the standard Fmoc solid-phase peptide chemistry as described previously (18). Fmoc protected L-amino acids were used and the following side chain protection was used: Boc (Lys), But (Ser, Thr), OBut (Asp, Glu), Trt (Asn, Cys, Gln, His), and Pbf (Arg). A test cleavage was performed after each five residues were coupled and the desired product was confirmed by MALDI-TOF mass spectrometry. Each test peptide was cleaved from the resin with a mixture of 87.5% TFA, 5% phenol, 5% water, 2.5% DTT, and 2.5% anisole for 90 minutes at room temperature with mechanical shaking.

After complete assembly of the peptide on the resin, the N-terminus was biotinylated by addition of biotin (0.5 mmol), DIC (0.5 mmol), and HOBT (0.5 mmol) in DMF to the resin. The suspension was allowed to stir for 27 hours at room temperature. Kaiser test was carried out to ensure complete biotinylation. The biotinylated peptide was released from support, with concomitant removal of acid-labile side chain protecting groups using the same procedure as used for the test cleavages. The filtrate from the cleavage reactions was collected, combined with TFA washes (3 x 2 min, 1 mL), and concentrated *in vacuo*. Cold diethyl ether (~ 15 mL) was added to precipitate the crude cleaved peptide. After trituration for 2 min, the peptide was collected upon centrifugation and decantation of the ether. The crude peptide was dissolved in 10-20% aqueous acetonitrile and purified on a semi-preparative VYDAC C18 reversed-phase HPLC column (10 x 250 mm, 5 μm) using an acetonitrile/water (in the presence of 0.05% TFA, v/v) gradient (flow rate = 2 mL/min, monitored at 220 nm) over a period of 40 minutes. The details of the gradient elution method used for purification of each peptide are listed in the Table 1. Purity of the peptides was confirmed by analytical reversed-phase HPLC and MALDI-TOF mass spectrometry (Table 1).

Table 2: The HPLC purification details for peptides **1**-**5**.

E2 Expression and Purification

Human embrionic kidney (HEK) 293 cells were cultured in high-glucose Dulbecco's modified Eagle's medium (DMEM) supplemented with 10% (v/v) fetal bovine serum at 37 °C in a humidified 5% CO_2 atmosphere. Transfections using the E2N2661 plasmid vector (29) were performed in 6 well tissue culture plates with 20 μg DNA per well using lipofectamine2000

reagent (Invitrogen) as per manufacturer's instructions. The cells were transfected at a density of 1.5 x 10^5 cells per 0.6 mL per well and harvested two days after transfection at about 90% confluence in ice-cold lysis buffer [50 mM Tris pH 7.0, 1 M NaCl and 1 mM phenylmethylsulfonyl fluoride (PMSF) as protease inhibitor]. After centrifugation, the supernatant containing protein lysate was loaded onto 12% SDS-PAGE gel. Prior to loading on the gels, the samples were treated by heating at 95 ˚C for 5 minutes in sample loading buffer (80 mM Tris-HCl, pH 6.8, 2% SDS, 10% glycerol, 2% β–mercaptoethanol, 0.02% bromophenol blue). Gel-separated proteins were electroblotted onto nitrocellulose membrane and the membrane was blocked overnight at 4 °C in 5% skim milk. The membrane was washed with TBST followed by incubation with the mouse anti-His_6 MAb (1:1000) or anti-E2 mAb (1:20) for 1 h. Subsequently the membrane was washed with TBST and incubated with goat anti-mouse horseradish peroxidase-linked secondary antibodies GAM–HRPO (1:10,000) for 1 h. Following a final washing step, the binding of MAbs to antigen was detected using the enhanced chemiluminescence substrate (ECL).

The crude cell lysate (CL) containing the His-tagged E2 protein was purified by immobilized metal affinity chromatography (IMAC) using a Ni^{2+}-NTA resin column under denaturing conditions according to the protocol provided by the manufacturer (Qiagen). Briefly, CL was incubated with Ni^{2+}-NTA resin, and the suspension was incubated overnight at 4 °C with gentle rocking. The resin was loaded on a column and equilibrated with 10 bed volumes of the lysis buffer (50 mM Tris–HCl, 1 M NaCl, pH 7.0). It was then washed extensively with the washing buffers containing increasing amounts of imidazole in the buffer. Finally, His-tagged protein was eluted using elution buffer (50 mM Tris–HCl, 1 M NaCl, and 300 mM imidazole, pH 7.0). The pure protein and the CL were analyzed by SDS-PAGE and Western blot as

described above. The concentration of the purified E2 was determined by the method of Lowry *et al.* using bovine serum albumin (BSA) as standard.(32) Duplicates were prepared for both the standards and the experimental samples. Experimental samples consisted of 50 μL of the purified E2 protein.

Biotin-Streptavidin based Binding Assay

A biotin-streptavidin based binding assay was developed to examine the binding affinity between the E2 protein and peptide ligands. E2 (N strain) antigen (100 μL, 150 or 200 ng/well) in PBS (1 mM, pH 7.4) was added to the wells of a 96-well microtiter immunoplate and incubated overnight at 4 °C to allow the antigen to adsorb to the surface. Excess antigen was removed from the plate by rinsing each well with 300 μL PBS (1 mM, pH 7.4) containing 0.05% Tween-20. Subsequently the wells were blocked by incubating with 200 μL of 2% BSA in PBS. After discarding the supernatant, each well was washed with 0.05% Tween-20 in PBS. Stock solutions of peptides **1**-**5** were prepared and concentrations were determined by Lowry assay.(32) Biotin was used as a control. Peptide solution or biotin (100 μL/well) was added to each well in duplicates and the plate was incubated at room temperature on a shaker (200 rpm) for 3 h. The supernatant was discarded and the wells were rinsed with 0.05% Tween-20 in PBS. To each well was then added a solution (100 μL) of Strep-HRPO (0.1 μg) in 1% BSA and the plate was incubated at room temperature for 1 h while gently agitating on a shaker. After discarding the Strep-HRPO solution, plate was rinsed with 0.05% Tween-20 in PBS (300 μL x 3) and TMB substrate solution (100 μL, TMB Peroxidase:Peroxidase solution B, 1:1, v/v) was added to each well. The plate was then incubated at room temperature for about 15 minutes until the absorbance reached an appropriate level (0.7-0.8). The absorbance in each well was

measured using ELISA V_{max} kinetic microplate reader (Molecular Devices Corp., CA, USA) at 650 nm. The equilibrium absorbance data for each peptide was plotted against peptide concentration. For peptides **3** and **5**, the absorbance data was fitted to Scheme 1 using the numerical simulation/least-squares fitting program Dynafit (21).

Circular Dichroism (CD) Spectroscopy

All CD measurements were made on an Olis CD spectrometer (Georgia, USA) at 25 °C in a thermally controlled quartz cell with a 0.02 cm path length over 190-260 nm. The peptide stock solutions were diluted with phosphate buffer (1 mM, pH 7.0) to give final concentrations of 25, 50, and 100 μM for CD measurements. Data were collected every 0.05 nm and were the average of 10 scans. The bandwidth was set at 1.0 nm and the sensitivity at 50 mdeg, and the response time was 0.25 s. In all cases baseline scans of aqueous buffer were subtracted from the experimental readings. Results were expressed in units of molar ellipticity per residue (deg cm^2 $dmol^{-1}$) and plotted versus wavelength. Analysis of the CD spectra involved quantitative curve fitting using the CDPro software analysis program (24) as described previously (18). Briefly, the software uses three programs to perform the protein secondary structure analysis from CD spectra. Output data from each of the three programs provide fractions of six different secondary structure classes, namely regular α-helix, distorted α-helix, regular β-strand, distorted β-strand, turns, and unordered. Since the same set of reference protein was used by each of the three programs, their fractional secondary structures could be averaged. For convenience of data interpretation, the regular and distorted components of α-helix and β-strand, and turns and unordered structural elements were added to give overall helical, strand, and coil structures, respectively. The final secondary structure elements were the average from the triplicate

samples for each peptide and the standard error was calculated for each of them. Each was also examined separately using the three analysis programs mentioned above and the standard error was calculated for each of them. The latter results are all within the experimental error given.

Acknowledgements

We are grateful to Istituto di Ricerche di Biologia Molecolare P. Angeletti, Rome, Italy for kindly providing the E2N2661 plasmid vector. We thank Dr. Petr Kuzmic for helpful discussions during curve fitting. We also thank Sahar Ahmed and Dr. Dipankar Das for helpful assistance and discussions.

References

1. Manns MP, Foster GR, Rockstroh JK, Zeuzem S, Zoulim F, Houghton M. (2007) The way forward in HCV treatment--finding the right path. Nat Rev Drug Discov;6:991-1000.
2. WHO. (2007) (World Health Organization). Initiative for Vaccine Research. Hepatitis C. WHO web site [online], <http://www.who.int/vaccine_research/diseases/viral_cancers/en/index2.html>.
3. Chevaliez S, Pawlotsky JM. (2007) Hepatitis C virus: virology, diagnosis and management of antiviral therapy. World J Gastroenterol;13:2461-6.
4. Manns MP, Wedemeyer H, Cornberg M. (2006) Treating viral hepatitis C: efficacy, side effects, and complications. Gut;55:1350-9.
5. Parfieniuk A, Jaroszewicz J, Flisiak R. (2007) Specifically targeted antiviral therapy for hepatitis C virus. World J Gastroenterol;13:5673-81.
6. Flisiak R, Dumont JM, Crabbe R. (2007) Cyclophilin inhibitors in hepatitis C viral infection. Expert Opin Investig Drugs;16:1345-54.
7. Dimitrov DS. (2004) Virus entry: molecular mechanisms and biomedical applications. Nat Rev Microbiol;2:109-22.
8. Meanwell NA. (2006) Hepatitis C virus entry: an intriguing challenge for drug discovery. Curr Opin Investig Drugs;7:727-32.
9. Cocquerel L, Voisset C, Dubuisson J. (2006) Hepatitis C virus entry: potential receptors and their biological functions. J Gen Virol;87:1075-84.
10. Cao J, Zhao P, Miao XH, Zhao LJ, Xue LJ, Qi Zt Z. (2003) Phage display selection on whole cells yields a small peptide specific for HCV receptor human CD81. Cell Res;13:473-9.

11. VanCompernolle SE, Wiznycia AV, Rush JR, Dhanasekaran M, Baures PW, Todd SC. (2003) Small molecule inhibition of hepatitis C virus E2 binding to CD81. Virology;314:371-80.
12. Wagner CE, Mohler ML, Kang GS, Miller DD, Geisert EE, Chang YA, et al. (2003) Synthesis of 1-boraadamantaneamine derivatives with selective astrocyte vs C6 glioma antiproliferative activity. A novel class of anti-hepatitis C agents with potential to bind CD81. J. Med. Chem.;46:2823-33.
13. Pecheur EI, Lavillette D, Alcaras F, Molle J, Boriskin YS, Roberts M, et al. (2007) Biochemical mechanism of hepatitis C virus inhibition by the broad-spectrum antiviral arbidol. Biochemistry;46:6050-9.
14. Bertaux C, Daelemans D, Meertens L, Cormier EG, Reinus JF, Peumans WJ, et al. (2007) Entry of hepatitis C virus and human immunodeficiency virus is selectively inhibited by carbohydrate-binding agents but not by polyanions. Virology;366:40-50.
15. Helle F, Wychowski C, Vu-Dac N, Gustafson KR, Voisset C, Dubuisson J. (2006) Cyanovirin-N inhibits hepatitis C virus entry by binding to envelope protein glycans. J Biol Chem;281:25177-83.
16. Nozaki A, Ikeda M, Naganuma A, Nakamura T, Inudoh M, Tanaka K, et al. (2003) Identification of a lactoferrin-derived peptide possessing binding activity to hepatitis C virus E2 envelope protein. J. Biol. Chem.;278:10162-73.
17. Jameson GB, Anderson BF, Norris GE, Thomas DH, Baker EN. (1998) Structure of human apolactoferrin at 2.0 A resolution. Refinement and analysis of ligand-induced conformational change. Acta Crystallogr D Biol Crystallogr;54:1319-35.

18. Kaur K, Andrew LC, Wishart DS, Vederas JC. (2004) Dynamic relationships among type IIa bacteriocins: temperature effects on antimicrobial activity and on structure of the C-terminal amphipathic alpha helix as a receptor-binding region. Biochemistry;43:9009-20.
19. Rosa D, Campagnoli S, Moretto C, Guenzi E, Cousens L, Chin M, et al. (1996) A quantitative test to estimate neutralizing antibodies to the hepatitis C virus: cytofluorimetric assessment of envelope glycoprotein 2 binding to target cells. Proc Natl Acad Sci U S A;93:1759-63.
20. Wakita T, Taya C, Katsume A, Kato J, Yonekawa H, Kanegae Y, et al. (1998) Efficient conditional transgene expression in hepatitis C virus cDNA transgenic mice mediated by the Cre/loxP system. J Biol Chem;273:9001-6.
21. Kuzmic P. (1996) Program DYNAFIT for the analysis of enzyme kinetic data: application to HIV proteinase. Anal Biochem;237:260-73.
22. Kuzmic P, Hill C, Janc JW. (2004) Practical robust fit of enzyme inhibition data. Methods Enzymol;383:366-81.
23. Kaur K, Lan MJK, Pratt RF. (2001) Mechanism of inhibition of the class C beta-lactamase of Enterobacter cloacae P99 by cyclic acyl phosph(on)ates: Rescue by return. J. Am. Chem. Soc.;123:10436-43.
24. Sreerama N, Woody RW. (2000) Estimation of protein secondary structure from circular dichroism spectra: Comparison of CONTIN, SELCON, and CDSSTR methods with an expanded reference set. Anal. Biochem.;287:252-60.
25. Eisenberg D, Weiss RM, Terwilliger TC. (1982) The helical hydrophobic moment: a measure of the amphiphilicity of a helix. Nature;299:371-4.

26. Carver T, Bleasby A. (2003) The design of Jemboss: a graphical user interface to EMBOSS. Bioinformatics;19:1837-43.
27. Flint M, Maidens C, Loomis-Price LD, Shotton C, Dubuisson J, Monk P, et al. (1999) Characterization of hepatitis C virus E2 glycoprotein interaction with a putative cellular receptor, CD81. J Virol;73:6235-44.
28. Goffard A, Dubuisson J. (2003) Glycosylation of hepatitis C virus envelope proteins. Biochimie;85:295-301.
29. Yagnik AT, Lahm A, Meola A, Roccasecca RM, Ercole BB, Nicosia A, et al. (2000) A model for the hepatitis C virus envelope glycoprotein E2. Proteins-Structure Function and Genetics;40:355-66.
30. Abe K, Nozaki A, Tamura K, Ikeda M, Naka K, Dansako H, et al. (2007) Tandem repeats of lactoferrin-derived anti-hepatitis C virus peptide enhance antiviral activity in cultured human hepatocytes. Microbiol Immunol;51:117-25.
31. De Francesco R, Migliaccio G. (2005) Challenges and successes in developing new therapies for hepatitis C. Nature;436:953-60.
32. Lowry OH, Rosenbrough NJ, Farr AL, Randall RJ. (1951) Protein measurement with the Folin phenol reagent. J Biol Chem;193:265-75.

TABLES

Table 1: CD Analysis of the Secondary Structure Fractions of Peptides **1-5** in PBS at 25 °C

Peptide[a]	Number of residues	α-helix[b] ± SEM	β-sheet[b] ± SEM	coil[b] ± SEM
1	33	0.32 ± 0.03	0.20 ± 0.002	0.48 ± 0.03
2	27	0.12 ± 0.06	0.35 ± 0.04	0.53 ± 0.02
3	17	0.38 ± 0.04	0.15 ± 0.04	0.47 ± 0.05
4	33	0.34 ± 0.02	0.16 ± 0.01	0.51 ± 0.007
5	27	0.71 ± 0.01	0.05 ± 0.002	0.23 ± 0.009

[a] All samples were prepared three times in PBS (10 mM, pH 7.0). Samples were allowed to equilibrate for at least 10 min at 25 °C before taking CD scans.. [b]Secondary structure determination from CD data was done using CDPro software (24) as described in the Experimental Section.

Table 2: The HPLC purification details for peptides **1**-**5**.

Peptide	Mass $[M+H]^+$ Observed (Calcd.)	Solvent used for HPLC purification	Elution time (min)	Pure Yield
1	4040 (4039)	10-45% acetonitrile/H_2O	22.3	50%
2	3370 (3369)	30% acetonitrile/H_2O	12.8	55%
3	2249 (2249)	10-40% acetonitrile/H_2O	35.5	65%
4	3980 (3979)	20-65% acetonitrile/H_2O	33.1	56%
5	3309 (3309)	20-65% acetonitrile/H_2O	29.8	52%

FIGURE LEGENDS

Figure 1: (A) Three-dimensional structure of 33-residue lactoferrin-derived peptide (600-632 amino acids) obtained from the crystal structure of recombinant human lactoferrin (pdb 1CB6) (17). Structure is shown as a ribbon diagram highlighting the helical (red) secondary structure. (B) Amino acid sequence of the 33-residue lactoferrin-derived peptide. Helical residues are underlined.

Figure 2: Sequence of five lactoferrin-derived peptides synthesized and studied herein. Residues that are underlined indicate a change from the native lactoferrin sequence. Nle stands for norleucine and b denotes biotin covalently linked to the N-terminus of the peptides.

Figure 3: E2N purification: Western blot analysis of the fractions obtained from the IMAC column, probed with mouse anti-His6 (1:1000) (left) and mouse anti-E2 (1:20) (right) monoclonal antibodies. CL: crude lysate; FT: flow through; 3-8: fractions 3-8 obtained using the elution buffer.

Figure 4: Binding of E2 protein to peptides **3** (top) and **5** (bottom). Shown is absorbance of TMB substrate at 650 nm as a function of different peptide concentration. The symbols are experimental data points whereas the line was calculated by fitting the data to Scheme 1 as described in the text.

Figure 5: Binding of E2 protein to peptides **1** (Δ), **2** (□), and **4** (o). Shown is absorbance of TMB substrate at 650 nm as a function of different peptide concentration. The symbols are experimental data points whereas the line is drawn to guide the eye.

Figure 6: Edmundson α-helical wheel representation of peptide **5**. The solid curve indicates the polar/hydrophilic face and the dashed curve denotes hydrophobic face.

A

B

VVSRMDKVERLKQVLLHQQAKFGRNGSDCPDKF
600 632

Figure 1

Peptide	Amino acid sequence	Number of residues
native LF fragment	VVSRMDKVERLKQVLLHQQAKFGRNGSDCPDKF	33
1	b-VVSRNleDKVERLKQVLLHQQAKFGRNGSDCPDKF	33
2	b-KVERLKQVLLHQQAKFGRNGSDCPDKF	27
3	b-KVERLKQVLLHQQAKFG	17
4	b-VVSRNleDKVERLKQVLLHQQAKFGRNGADCPAKF	33
5	b-KVERLKQVLLHQQAKFGRNGADCPAKF	27

+

Figure 2

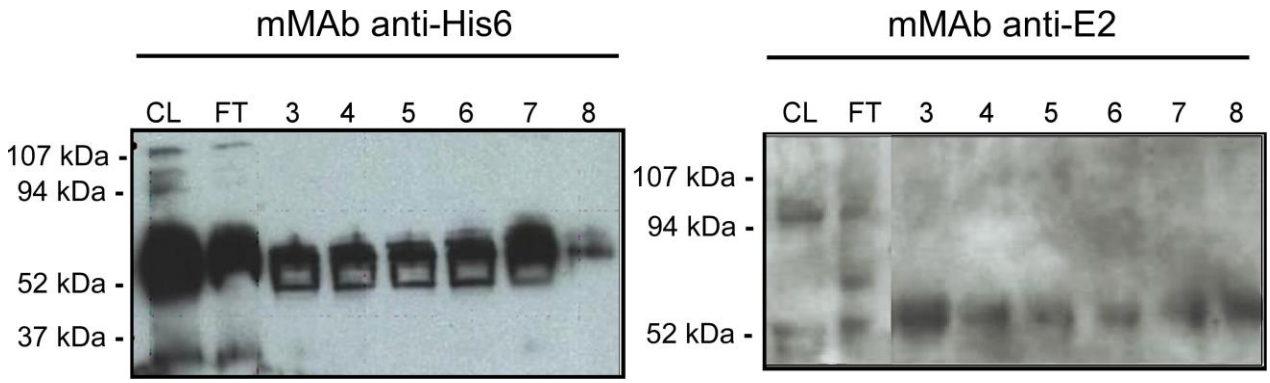
mMAb anti-His6
CL FT 3 4 5 6 7 8
107 kDa
94 kDa
52 kDa
37 kDa
mMAb anti-E2
CL FT 3 4 5 6 7 8
107 kDa
94 kDa
52 kDa

Figure 3

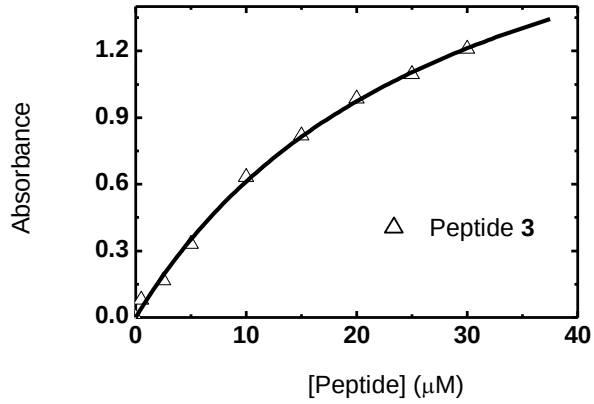
Absorbance
1.2
0.9
0.6
0.3
0.0
0
10
20
30
40
Peptide 3
[Peptide] (μM)

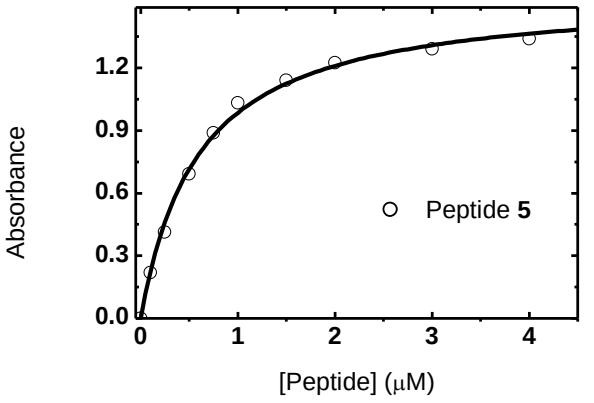
Absorbance
1.2
0.9
0.6
0.3
0.0
0
1
2
3
4
Peptide 5
[Peptide] (μM)

Figure 4

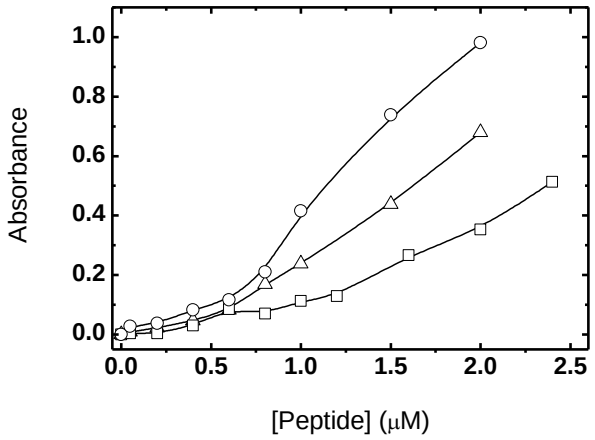

Figure 5

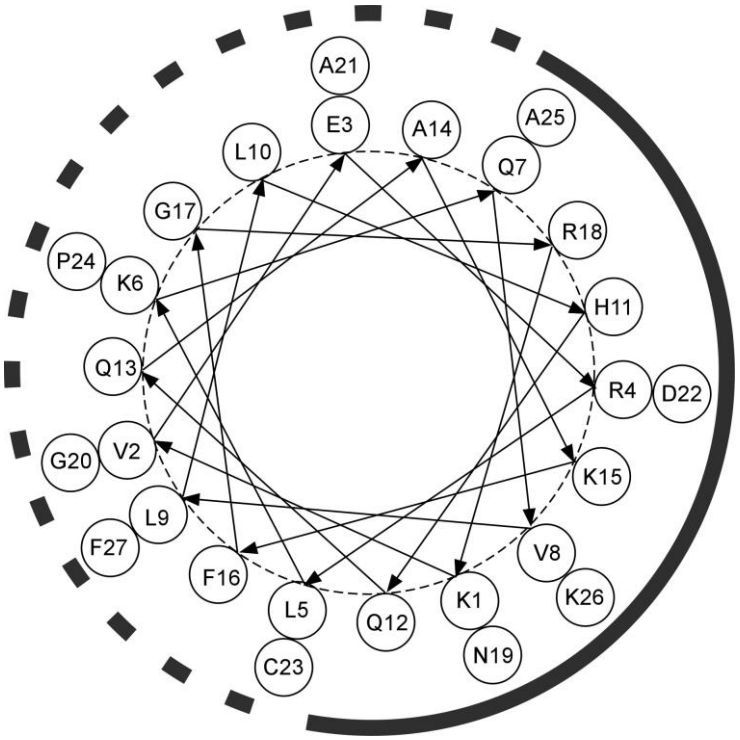
A21
E3
A14
A25
L10
Q7
G17
R18
P24
K6
H11
Q13
R4
D22
G20
V2
K15
L9
F27
V8
F16
K26
L5
Q12
K1
N19
C23

Figure 6